PHYSICAL REVIEW B VOLUME 17, NUMBER 8 15 APRIL 1978

Hall-mobility anisotropy in GaSe

V. Augelli, C. Manfredotti, R. Murri, and L. Vasanelli
Istituto di Fisica, Università di Bari, Bari, Italy
and Gruppo Nazionale di Struttura della Materia, Consiglio Nazionale delle Ricerche, Italy
(Received 7 November 1977)

The Hall mobility has been measured for the first time in a layer compound both along and perpendicular to the layers. The measurements have been extended as a function of temperature and of electrical field by a pulse technique. The results indicate that both mobilities are limited by homopolar optical-phonon scattering and that the effective conductivity masses for holes are different from those derived from time-of-flight measurements. Moreover, the Hall mobility along the *c* axis is evidently field dependent. It is concluded that stacking faults are responsible for the difference between low-field and high-field mobilities.

I. INTRODUCTION

GaSe, a typical layer compound, is characterized by strong structural anisotropy with respect to one crystal axis: it consists of tightly bound four-atom layers which are stacked on top of each other. Until now, it has been impossible to fully investigate the optical and electrical anisotropy properties of GaSe, essentially because it is very difficult to obtain sufficiently thick samples along the *c* axis. The reason is that easy cleavage occurs parallel to the layers. For instance, while the carrier mobility has been extensively investigated along the layers,[1-3] the mobility along the *c* axis either has been estimated with indirect methods[4] or measured at high electric fields on very thin samples by using the time-of-flight technique.[5] In the present work, we succeeded in measuring directly and for the first time the Hall mobility of holes in GaSe both along and perpendicular to the layers. To our knowledge, this is the first direct determination of Hall mobility in a layered crystal along its anisotropy axis.

II. EXPERIMENTAL

Samples used in the present experiment were *p* type and were extracted from the same Bridgman ingot. Details of the growth technique are given elsewhere.[6] The samples were cut with a diamond saw in the form of rectangular parallelepipeds, with typical dimensions $2\times2\times7$ mm^3, the longest dimension being either parallel to the *c* axis or to the layer plane. Before cutting, samples were embedded in an acrylic resin, in order to be handled without damage. Surfaces perpendicular to the layers were finely polished with diamond paste: surface damage was kept to a minimum by reducing lapping pressure. Hall contacts were obtained by In evaporation in a vacuum better than 10^{-4} Torr: a short treatment at 150 °C under N_2 atmosphere improved the Ohmicity of the contacts. The stability and Ohmicity of these contacts did not depend on the surface (cleaved or polished) where they were evaporated. A conventional five-contact Hall geometry was used (see Fig. 1): the current contacts *A* and *D* extended over the two bases, while the voltage contacts *B*, *C*, and *E* were in form of strips 0.3 mm wide, perpendicular to the current flow. The contacts *B* and *C*, which were about 1.5 to 2 mm apart, were used also for measuring the resistivity by disconnecting the potentiometer. All the dimensions, distances, etc. were accurately determined by an optical microscope. Because the length-to-width ratio of the samples was around 3.5, no correction was made for the shortening effect of large-area current contacts. The measurements were carried out as a function of temperature by means of a N_2 flux cryostat and in a 1.8-T magnetic field. Checks were made continuously in order to verify the independence of Hall coefficient and resistivity of the current intensity. Interfering thermoelectric and thermogalvanomagnetic effects were eliminated by reversing the current and the magnetic-field polarity. Checks of the independence of the Hall coefficient R_H from the magnetic field and the current intensity are shown in Figs. 2(a) and 2(b).

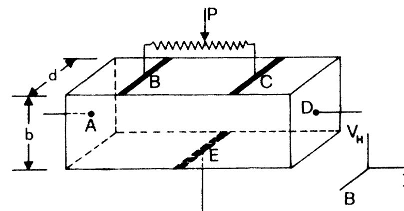

FIG. 1. Five-contact geometry used for Hall measurments. The directions of the current I, of the magnetic field B, and of the measured Hall tension V_H are shown on the right.

 © 1978 The American Physical Society

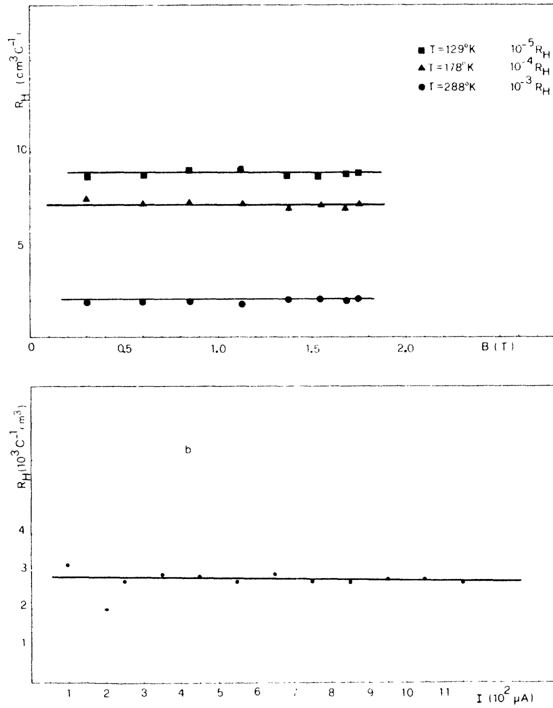

FIG. 2. Check of the independence of the Hall coefficient R_H from: (a) the magnetic field B and (b) the current intensity I. The current is flowing (a) perpendicular and (b) parallel to the c axis.

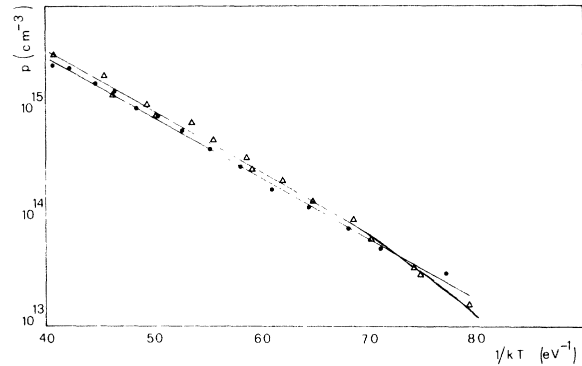

FIG. 3. Behavior of hole concentration as a function of $1/kT$ as obtained from Hall measurements along the c axis (△) and along the layers (●).

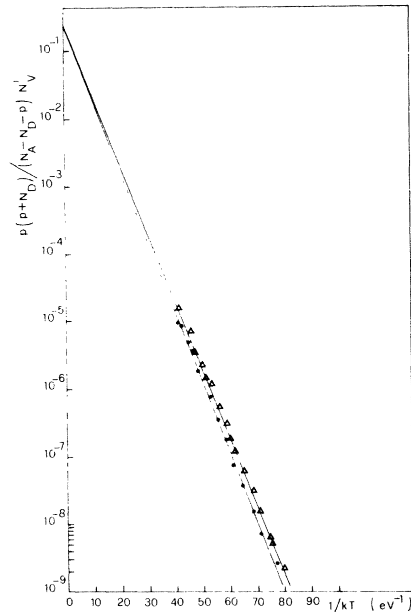

FIG. 4. Single-donor–single-acceptor model analysis of experimental data parallel (△) and perpendicular (●) to c axis, shown in Fig. 3. Full lines represent the best fits. In the expression reported along the vertical axis $N_V' = (m_h^*/m_e)^{3/2} N_V$ with N_V the density of states in the valence band, m_h^* the effective mass of holes, and m_e the free-electron mass.

III. RESULTS

From the Hall coefficient R_H, assuming as usual that the ratio of Hall to drift mobility is equal to one, holes concentrations have been calculated. Since the samples were extracted from near portions of the same ingot, the hole concentration turned out to be approximately the same for Hall measurements along the c axis as well as along the layers. The behavior of hole concentrations as a function of temperature in both directions is shown in Fig. 3.

The single-donor–single-acceptor model[7] was used for data analysis by assuming the usual three-dimensional expression for the density of states. The fitting was carried out with a special high-convergence minimization program based on the χ^2 method. The results are shown in Fig. 4 for all measurements along the c axis and along the layers. The parameters obtained by this fit are acceptor (N_A) and donor (N_D) concentrations and activation energy of the acceptor level (E_A); they are listed in Table I together with their errors and with the confidence level (C.L.) of the fit. The density-of-states effective mass for the valence band was taken equal to $0.5m_e$.[8]

The fact that in both directions the parameters are practically the same and coincide with those previously reported (see Ref. 8, sample R4, obtained from the same ingot) can be considered as a good check for the present measurements, particularly for those carried out along the c axis. The behavior of the hole mobility along and perpendicular to the c axis as a function of temperature is displayed in Fig. 5. Around room temperature, the curves have been fitted by the relation

TABLE I. Values of the parameters obtained from the single-donor–single-acceptor model analysis shown in Fig. 4. N_A and N_D are the acceptor and donor concentrations, respectively, E_A is the acceptor ionization energy, and C.L. the confidence level of the fitting. Standard deviations are also given.

Direction	N_A (cm^{-3})	N_D (cm^{-3})	E_A (eV)	C.L.
$\perp c$	$(3.5 \pm 1.3) \times 10^{16}$	$(1.0 \pm 3.5) \times 10^{12}$	0.235 ± 0.006	65%
$\parallel c$	$(3.9 \pm 1.9) \times 10^{16}$	$(3.3 \pm 4.4) \times 10^{13}$	0.230 ± 0.009	40%

$$\mu(T) = \mu_0 (T/T_0)^{-n}, \quad (1)$$

where μ_0 is the room-temperature mobility and $T_0 = 300$ K. As one can note, the Hall-mobility anisotropy $\mu_{\perp\vec{c}}/\mu_{\parallel\vec{c}}$ is about 3.5 at room temperature.

For the analysis of these data, the model developed by Schmid,[9] which assumes short-range interactions with homopolar optical phonons polarized normally to the layers, has been used and the best fits are shown in Fig. 5.

While there was no problem concerning the mobility along the c axis, in the case of the mobility along the layers one had to choose between the best fits closer to experimental points at high or at low temperatures. Our choice seems to be the most physical one, since at low temperature a small contribution from ionized-impurity scattering is certainly present. In the best fit, the values of the phonon energy ($\hbar\omega$) and of the product between the coupling constant g^2 and the hole-conductivity mass m_c have been used as parameters, and the obtained values are listed in Table II.

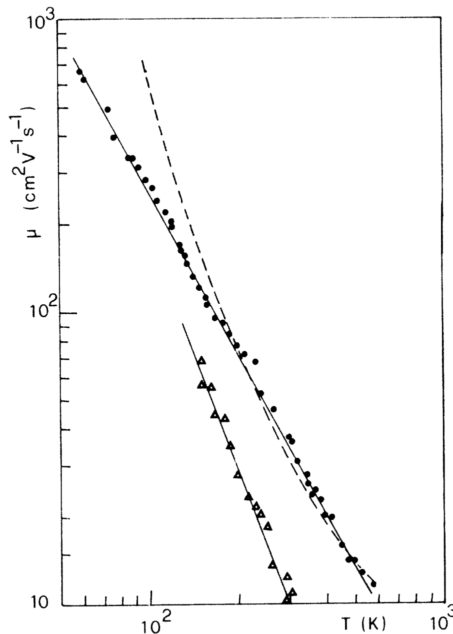

FIG. 5. Behavior of the Hall mobility along the c axis (Δ) and perpendicular to c axis, ($\bullet$). The fit with expression (1) gives values of $n = 2.67$ and $n = 1.85$, respectively, (full lines). The fit with Schmid's model (slashed lines) gives values of the parameters which are reported in Table II. In the case of the mobility along the c axis the two fits practically coincide.

The coupling constant between holes and phonons is given by

$$g^2 = \mathcal{E}^2 m_h^{3/2} / 2\sqrt{2}\,\pi\hbar M N (\hbar\omega)^{3/2}, \quad (2)$$

where $\mathcal{E}$ is the deformation potential for the valence band with respect to the normal coordinates of the phonon involved, m_h is the density-of-states effective mass for the valence band, M is a reduced ionic mass, and N the number of cells per unit volume.

In the evaluation of m_c and $\mathcal{E}$, the hypothesis has been made of a constant g^2 value in the two directions.

The Hall mobilities along and perpendicular to the c axis have been measured on the same samples by a pulse technique in order to investigate the behavior of the mobility at relatively high electric fields. The measurements were carried out at room temperature by applying square-voltage pulses 100 μsec in length, with 20-Hz repetition frequency, and up to 500 V in height. The Hall-voltage pulses were revealed with an oscilloscope with a differential plug in. Contact instabilities prevented the electric fields from exceeding 500 V/cm and caused estimated experimental errors of about 10%. The results are shown in Figs. 6(a) and 6(b). The behaviors are completely different:

TABLE II. Values of the parameters obtained by a best fit of the curves shown in Fig. 5 with Schmid's model: phonon energy, ($\hbar\omega$); (coupling constant) × (hole conductivity mass), ($g^2 m_c$); hole conductivity mass, (m_c); and deformation potential ($\mathcal{E}$).

Direction	$\hbar\omega$ (meV)	$g^2 m_c$	m_c	$\mathcal{E}$ (eV/Å)
$\parallel c$	13.8	$0.69 m_e$	$1.18 m_e$	9.4
$\perp c$	11.5	$0.19 m_e$	$0.32 m_e$	8.1

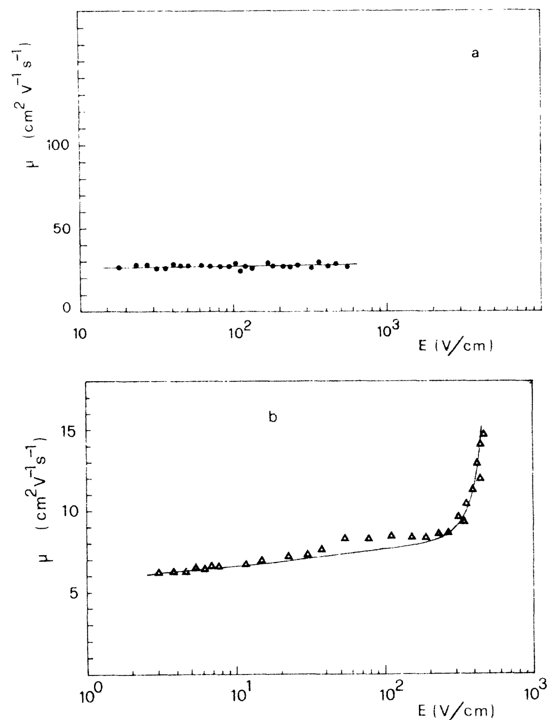

FIG. 6. Hall mobility as a function of electric field measured by pulse technique (a) along the layers and (b) perpendicular to the layers.

the Hall mobility along the layers is constant up to 500 V/cm, while the mobility along the c axis increases quite steeply at about $E = 350$ V/cm. It can be noted that the mobility anisotropy ratio $\mu_{\perp\vec{c}}/\mu_{\parallel\vec{c}}$ at room temperature and low electric fields is the same as that obtained in dc measurements. Finally, the behavior of $\rho_{\parallel\vec{c}}$ and $\rho_{\perp\vec{c}}$ in dc conditions was measured as a function of temperature and displayed in Fig. 7.

Since both curves show the same activation energy, one can conclude that the resistivity anisotropy is independent of temperature, in agreement with previous results obtained by direct measurements of the resistivity anisotropy.[10]

IV. DISCUSSION

Previously,[5] measurements of the drift mobility μ_d of holes along the c axis have been carried out with the time-of-flight technique, giving a value of μ_d at room temperature of about 215 cm^2 V^{-1} sec^{-1}, which is much higher than the value quoted in the present work ($\mu_H = 8$ to 10 cm^{2}V^{-1} sec^{-1}). Since there are no reasons for assuming a value of $r = \mu_H/\mu_d$ much different from 1, the only justification for this disagreement should lie in the fact that our measurements are performed at electric fields much lower than those needed by the time-of-flight technique (10^4 to 10^5 V/cm). Now, since it has been proved that our Hall mobility is a true lattice mobility (see Fig. 5), it is clear that the strong increase of the mobility from low to high fields cannot be attributed to the disappearance of some extrinsic scattering mechanism.[5] More likely, since the behavior of the Hall mobility above 300 V/cm is compatible with a tunneling mechanism, i.e., $\mu \propto e^{-b/V}$, the same increase could be attributed to the tunneling through some potential barriers due to the evident disorder existing along the c axis.

Since the acceptor energies, evaluated by applying the single-donor–single-acceptor model to Hall measurements as a function of temperature are exactly the same, one can conclude that conduction in both directions occurs in the same valence band and, therefore, one can obtain information concerning the anisotropy of the valence band around the minimum. The mobility curves can be analyzed according to a theory[9] which assumes that the deformation-potential scattering by optical phonons should be very important in covalent crystals with

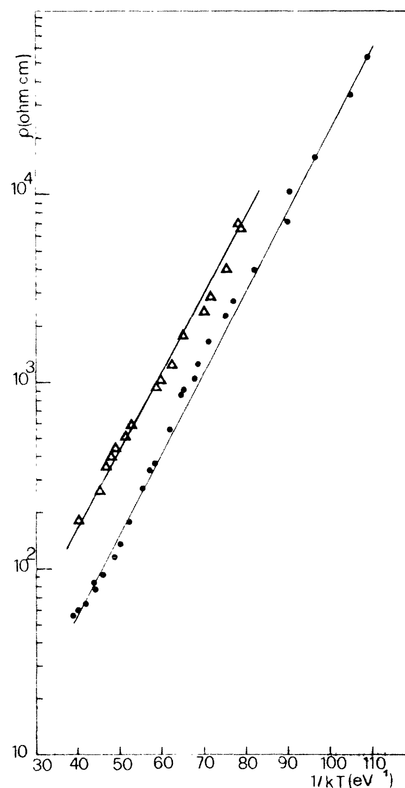

FIG. 7. Behavior of the electrical resistivity along the c axis (Δ) and perpendicular to the c axis (●) as a function of temperature.

TABLE III. Comparison between the results obtained in the present work and those reported previously [Refs. (1, 5, 13)]. In this table, $m_{\parallel \mathscr{E}}$ and $m_{\perp \mathscr{E}}$ are the conductivity effective masses for the valence band along and perpendicular to the c axis, g^2 is the electron-phonon coupling constant, and $\mathscr{E}$ is the deformation potential for the valence band.

	$m^*_{\parallel c}/m_e$	$m^*_{\perp c}/m_e$	g^2	$\mathscr{E}$ (eV/Å)	$g^2 m_{\parallel c}/m_e$	$g^2 m_{\perp c}/m_e$	$m_{\parallel c}/m_{\perp c}$
Present work	1.18	0.32	0.59	9.4($\parallel c$) 8.1($\perp c$)	0.69	0.19	4
Ref. 1	···	0.44	0.38	11.0	···	0.17	···
Refs. 5 and 13	0.2	0.8	0.25	6.6	···	0.2	0.25

low-site symmetry as in GaSe. As a matter of fact, the values of n are appreciably larger than 1.5 in both directions (see Fig. 5). The relevant phonons should be fully symmetric A_1' modes polarized normally to the layers. Looking at Table II in which the results of the fit of the mobility curves are reported, one can note a slight difference between phonon energies which at present is not completely understood and which gives rise to certain discrepancies between the values of $\mathscr{E}$. Tentatively one can assume that impurity scattering or, more likely, structural-defect scattering such as stacking faults and dislocations, which should act differently in the two directions, could be responsible for the observed discrepancy.

Raman, infrared, and neutron-scattering measurements[11-13] indicate energies of 38.1 meV for the $A_1'^{(2)}$ mode, 16.7 meV for the $A_1'^{(1)}$ mode, and 4.6 meV for A_2''(ir) mode.

Clearly, in the temperature range of the present experiment, the first mode cannot affect the Hall mobility and, taking into account our results, the last two modes should be active in carrier scattering.

In other words, both rigid-layer modes in which adjacent layers vibrate rigidly out of phase and modes in which in the same layer Ga and Se atoms vibrate out of phase should be present limiting the carrier mobility. Incidentally, if one uses the force-constant model proposed in the same reference one obtains for the $A_1'^{(1)}$ mode a deformation potential $\mathscr{E} \simeq 8$ eV/Å, which compares reasonably well with our values.

A general comparison between our results and those quoted in Refs. 1, 5, and 14 is presented in Table III. The disagreement between our results and those quoted in Refs. 5 and 14 has been already explained as due to different electric field ranges. Looking at Fig. 6(b) the reasonable hypothesis can be made that the increase of the mobility along the c axis as a function of the electric field should lead to the high mobility values measured with the time-of-flight technique at large enough electric fields. The reason that there are two different mobilities, at low and high electric fields, respectively, both dominated by the same scattering mechanism and both Ohmic, is not easy to explain. The most likely possibility is that stacking faults which make GaSe disordered to some extent along the c axis affect the shape of the top of the valence band. In practice, this effect can be pictured as an increase of the conductivity effective mass along the c axis with respect to that of a perfect crystal. Since stacking faults act as potential barriers or, better, they give rise to small oscillations in the energy of the top of the valence band, their effect disappears at high enough electric fields. In this sense, one can conclude that the conductivity effective mass depends in fact on the electric field, and that there is a range of electric fields between 5×10^2 and 5×10^3 V/cm roughly in which the effect of stacking faults diminishes quite rapidly. Clearly, our view is different from that introduced in Ref. 15, since we do not observe either hopping mobility along the c axis or activation energies in the behavior of the resistivity anisotropy as a function of temperature. If our picture is right, it should not be possible to determine the conductivity effective masses at high fields, as in Ref. 5, by using a density-of-states effective mass $m^* = 0.5m_e$ determined at low fields. In this sense, the entire last row of Table II must be evaluated again, by measuring directly the effective mass at high electric fields.

The possibility which has been discussed so far is not the only one; another one could exist which assumes a strong difference between Hall and drift mobility. This is likely in a disordered semiconductor in which the band width is large enough.[16] However, since in our case the mobilities are not exactly low and are not thermally activated, this possibility must be rejected. The only way to overcome this impasse is to measure directly the Hall mobility at high electric fields and also to develop a band theory which takes into account potential barriers given by stacking faults.

Finally, in view of what was discussed above, a certain agreement between our results and those obtained previously by Fivaz and Mooser[1] is not surprising on the basis of a two-dimensional model.

V. CONCLUSION

The Hall effect has been measured for the first time on a layer compound. The validity of the results is supported by the good agreement on the value of the energy of the dominant acceptor obtained in both the Hall measurements along and perpendicular to the *c* axis. Homopolar optical phonons involving both out-of-phase rigid-layer modes and out-of-phase Ga-Ga vibrations seem to be responsible for hole scattering in both cases. The values of the coupling constant and of the deformation potential are larger than previously reported, but they are in better agreement with a reasonable estimate based on a proposed force-constant model. Measurements as a function of the electric field indicate that the Hall mobility along the *c* axis is field dependent starting from about 350 V/cm. The conductivity masses of valence-band holes are different from those evaluated by time-of-flight measurements, but they are more consistently calculated from all low-field data. The behavior of the hole transport properties along the *c* axis is to some extent similar to that for a disordered crystal, even if hopping mechanisms can be excluded on the basis of present measurements.

In our opinion, stacking faults are responsible for a modification of the shape of the top of the valence band in the [001] direction, which is reflected by an increase of the conductivity mass in the same direction.

ACKNOWLEDGMENT

This work was partially supported by National Council of Research.

[1]R. Fivaz and E. Mooser, Phys. Rev. 163, 743 (1967).
[2]F. I. Ismailov, C. A. Akundov, and O. R. Vernich, Phys. Status Solidi 17, K237 (1966).
[3]C. Tatsuyama, C. Hamagouchi, H. Tomita, and J. Nakai, Jpn. J. Appl. Phys. 10, 1698 (1971).
[4]Ph. Schmid and E. Mooser, Helv. Phys. Acta 45, 870 (1972).
[5]R. Minder, G. Ottaviani, and C. Canali, J. Phys. Chem. Solids 37, 417 (1976).
[6]V. L. Cardetta, A. M. Mancini, and A. Rizzo, J. Cryst. Growth 16, 183 (1972).
[7]J. S. Blakemore, *Semiconductor Statistics* (Pergamon, New York, 1962), p. 117.
[8]C. Manfredotti, A. M. Mancini, R. Murri, A. Rizzo, and L. Vasanelli, Nuovo Cimento B 39, 257 (1977).
[9]Ph. Schmid, Nuovo Cimento B 21, 258 (1974).
[10]V. Augelli, C. Manfredotti, R. Murri, A. Rizzo, and L. Vasanelli (unpublished).
[11]T. J. Wieting and J. L. Verble, Phys. Rev. B 5, 1473 (1972).
[12]J. L. Brebner, S. Jandl, and B. M. Powell, Solid State Commun. 13, 1555 (1973).
[13]E. Finckman and A. Rizzo, Solid State Commun. 15, 1841 (1974).
[14]Ph. Schmid and J. P. Voitchovsky, Phys. Status Solidi B 65, 249 (1974).
[15]K. Maschke and Ph. Schmid, Phys. Rev. B 12, 4312 (1975).
[16]P. G. Le Comber, and J. Mort, *Electronic and Structural Properties of Amorphous Semiconductors* (Academic, New York, 1973), p. 369.